Ultrasonic Metal Welding Process Robustness in Aluminum Automotive Body Construction Applications

Process robustness to four key manufacturing variables — weld orientation, aluminum sheet rolling direction, residual stamping lubricant level, and material age — was established

BY E. T. HETRICK, J. R. BAER, W. ZHU, L. V. REATHERFORD, A. J. GRIMA, D. J. SCHOLL, D. E. WILKOSZ, S. FATIMA, and S. M. WARD

ABSTRACT

Ultrasonic metal welding is a promising joining method for aluminum automotive body construction applications. In order to achieve technology implementation readiness, process robustness to weld orientation, aluminum sheet rolling direction, residual stamping lubricant level, and material age must be assessed. Experiments were conducted to characterize variations in weld failure loads and microstructural features resulting from the directional nature of the energy input during ultrasonic welding to ensure that the angle at which components are ultrasonically welded together does not affect weld performance. These experiments were also designed to ascertain whether the orientation of a welding machine with respect to the rolling lines on an AA6111 sheet component or the relative orientation of the rolling directions of two components being joined is critical. A second set of experiments was conducted to determine the effects of surface lubricant level on tensile-shear and T-peel failure loads and fatigue performance for AA6111 and AA5754 sheet. Robustness to surface lubricant level is important because often in North American automotive production facilities, components are not cleaned prior to welding; rather, they are welded with residual stamping lubricant on the surfaces. Finally, because AA6111 naturally ages at room temperature for an extended period of time in the T4 temper, experiments were performed to ascertain the impact of AA6111 material age on ultrasonic weld tensile-shear and T-peel failure loads. For all factors considered in this study, ultrasonic metal welding process robustness was demonstrated.

Introduction

Ultrasonic metal welding is a novel and promising joining technique for automotive body construction applications. It is a solid-state welding process that produces coalescence through the simultaneous application of localized high-frequency vibratory energy and moderate clamping forces. Ultrasonic metal welding requires significantly less energy than competing processes such as resistance spot welding; has variable costs an order of magnitude lower than self-pierce riveting; and is characterized by low heat input, thereby alleviating issues related to part distortion, aluminum alloy property degradation, and part handling safety. In addition, the performance of aluminum ultrasonic spot welds compares favorably with that of other types of joints both under quasi-static and dynamic loading (Ref. 1).

Ultrasonic spot welding systems include wedge-reed, lateral-drive, and torsion configurations. In all of the systems, ultrasonic vibration is generated by one or more transducers, which convert the high-frequency electrical energy generated by the power supply into mechanical vibratory energy of the same frequency. This vibration is transmitted through a sonotrode into the workpieces, with tip vibration in a plane parallel to the plane of the weld interface. In the case of commercially available wedge-reed and lateral-drive systems, tip vibration is linear and in the same direction as transducer movement. In the case of torsion welding systems, a special arrangement of multiple transducers facilitates a reciprocating torsional motion of the sonotrode. For all of the aforementioned weld configurations, a static force is applied perpendicular to the plane of the weld interface to clamp the workpieces together between the sonotrode tip and the anvil. The frictional action between the workpiece surfaces as they are subjected to ultrasonic vibration and clamping pressure disperses interface oxides and contaminants and brings about metal-to-metal contact and bonding.

KEYWORDS

Ultrasonic Welding
Automotive
Aluminum

Ultrasonic metal welding equipment was developed in the 1940s and 1950s (Ref. 2) and was first patented in the United States in 1960 (Ref. 3). Traditional applications for ultrasonic metal welding include tube sealing, wire bonding, and thin foil joining. Ford Motor Co. and three joint venture partners — Branson Ultrasonics Corp., Edison Welding Institute, and Sonobond Ultrasonics Inc. — have recently concluded a four-year National Institute of Standards (NIST) Advanced Technology Program (ATP) (Ref. 4) to develop ultrasonic metal welding capability for aluminum closure and structural welding applications.

Lightweight materials such as aluminum allow automotive manufacturers to reduce vehicle weight to improve fuel economy and reduce CO_2 emissions. The principal barrier to the increased use of aluminum in automotive body and chassis applications is cost. Both the material cost and the body-in-white manufacturing cost are higher than that of steel. In order to achieve expanded use of aluminum in automotive body construction, lower-cost joining methods are important. Ultrasonic metal welding is one such potential joining method, but requisite to its implementation in automotive body

E. T. HETRICK, L. V. REATHERFORD, A. J. GRIMA, D. J. SCHOLL, D. E. WILKOSZ, and S. M. WARD are with Ford Motor Co. J. R. BAER is retired from Ford Motor Co. W. ZHU was formerly with Ford Motor Co., and is currently with U.S. Patent and Trademark Office. S. FATIMA was formerly with Ford Motor Co. and is currently with Wayne State University.

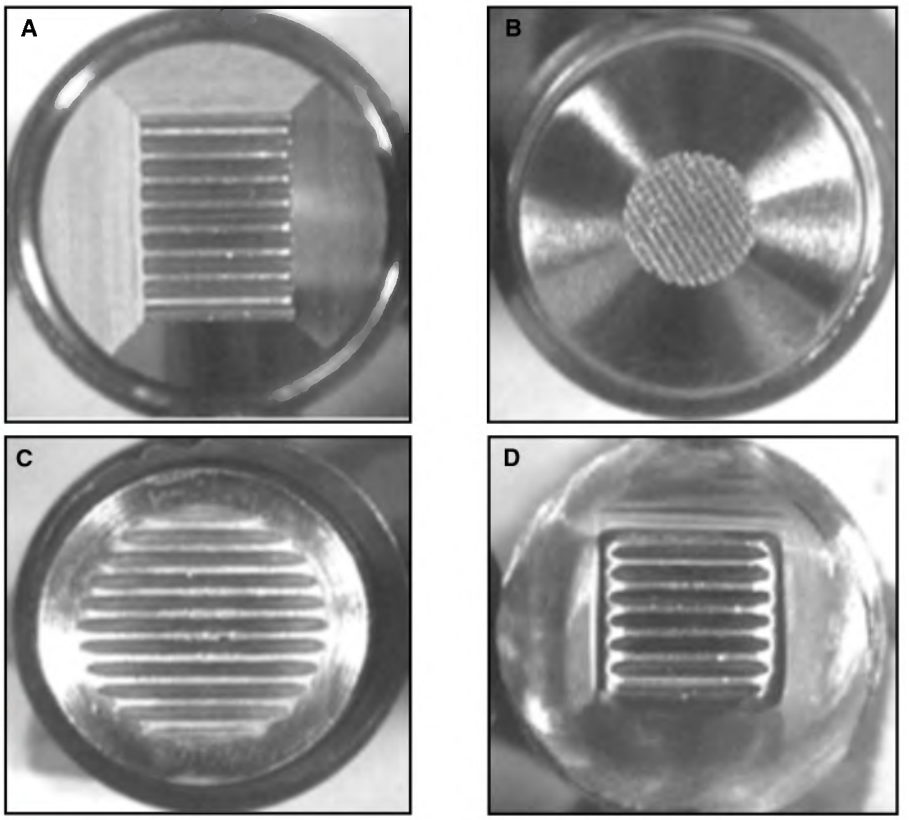

Fig. 1 — Typical sonotrode tip gripping surface patterns: A — Flat row; B — flat axisymmetric; C — spherical row; D — cylindrical row.

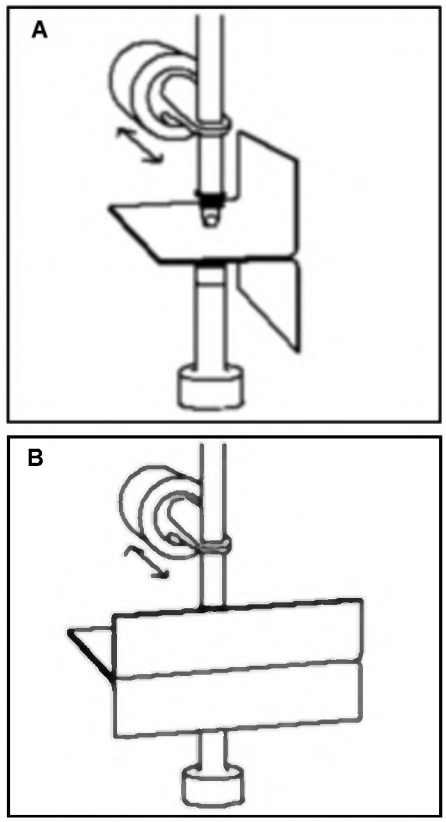

Fig. 3 — Test direction relative to vibration input direction – T-peel samples: A — Perpendicular; B — parallel.

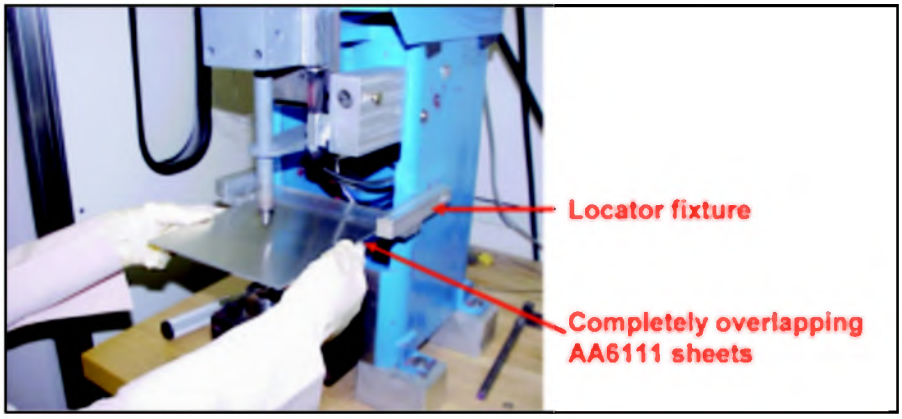

Fig. 2 — Welding setup for weld orientation and sheet rolling direction experiments.

construction applications is demonstration of process robustness to manufacturing variables. In this study, process robustness to four critical issues — weld orientation, aluminum sheet rolling direction, residual stamping lubricant level, and material age — was evaluated.

Robustness to Weld Orientation

Objective

In the case of linear welding systems, i.e., the wedge-reed and lateral-drive configurations, the energy input during ultrasonic welding is linear and in the same direction as transducer movement, so it is directional in nature. Prior work has indicated that this directional energy input might influence ultrasonic metal weld quality, but no studies have specifically addressed this issue. Tsujino et al. (Ref. 5) developed complex vibration longitudinal-torsional ultrasonic welding systems to ensure weld strength independence with respect to the angle between welding tip vibration and specimen loading orientation. Jones et al. (Ref. 6) investigated the fatigue strength of multi-weld aluminum panels as a function of vibration input direction, having noted a lack of symmetry in the surface marks left by the welding tip and the deformation at the interface. Their findings with regard to fatigue strength as a function of vibration input direction were inconclusive, however.

It was the objective of this study to determine whether welds made with linear ultrasonic metal welding systems were directional in nature or if they were independent of weld orientation. This is critical for ensuring that the angle at which components are ultrasonically welded together does not affect weld performance. In addition, the gripping surface pattern on many ultrasonic metal welding tips is nonaxisymmetric, as is shown in Fig. 1. As such, it was a second objective of this study to determine if tip geometry and gripping surface pattern affect the axial uniformity of weld properties.

Experimental Procedure

All welding was conducted using a Sonobond pedestal welding machine, as shown in Fig. 2. Welds were made on completely overlapping, 178-mm square sheets of 0.9-mm AA6111-T4. Square sheets were chosen such that all weldments presented identical vibratory conditions to the welding machine. All welding was conducted with a locator fixture to ensure consistent specimen orientation and location with respect

to the tip, as shown in Fig. 2. Four types of welding tips were used (shown in Fig. 1) — flat contact area with and without axisymmetric gripping surface patterns, spherical, and cylindrical (i.e., different radius of curvature side to-side than front to back). Different welding parameters were selected for each tip type, and all welding was conducted in an energy-controlled mode, with the power supply set to deliver a specified amount of energy but weld duration not inherently constrained.

A D-optimal designed experiment (DOE) was conducted to simultaneously evaluate the impact of weld orientation and aluminum sheet rolling direction (as detailed in the next section) on tensile-shear failure load, T-peel failure load, button size, weld time, and weld microstructure. A total of 288 welds were made — 12 replicates of 24 different combinations of factors. Five of the replicates were for testing in tensile-shear, five for testing in T-peel, and two for microstructural evaluation. For each weld, the voltage and current were measured at the power supply output, on the low-voltage (primary) side of the matching transformer. After welding, samples were bent to prescribed geometries for T-peel and tensile-shear testing, with T-peel and tensile-shear failure loads measured either parallel to or perpendicular to the vibration input direction, as is illustrated schematically in Figs. 3 and 4. Tensile-shear and T-peel testing were conducted using an Instron Model 4505 with a crosshead speed of 10 mm/min, with samples mounted as shown in Fig. 5.

Specimens for microstructural analysis were sectioned either parallel or perpendicular to the direction of vibration input, as shown in Fig. 6, using a medium-speed diamond cutoff wheel. Cross sections were cold mounted using a two-component epoxy resin, polished, etched, and examined with optical microscopy. For each weld cross section, 19 microstructural features were measured, as listed in Table 1 and shown in Fig. 7.

Results

In order to facilitate the consistent presentation of the results of this study with those of the subsequent three studies, results presented here focus on those specific to the flat row tip. DOE analyses indicated that the effect of changing test direction on tensile-shear and T-peel failure loads and button sizes was insignificant. Figure 8 plots mean failure load as a function of test direction (averaged across all other factors), with error bars corresponding to ±1 standard deviation. Figure 9 displays mean button size as a function of test type and test direction (averaged across all other factors), again with error bars corresponding to ±1 standard deviation. Note that button area, rather than button diameter, was used as the metric for button characterization. This method has been found to more accurately characterize the noncircular buttons that result frequently during ultrasonic metal welding due, in part, to noncircular tip geometries. Each bar in Figs. 8 and 9 represents the average of 15 welds. All eight data sets exhibited normality, and tensile-shear and T-peel failure load and button size data displayed equal variances and equal means at the 95% confidence level, respectively, as a function of test direction. As previously mentioned, it was therefore concluded that ultrasonic weld quasi-static strength is robust to weld orientation for 0.9-mm AA6111-T4 sheets joined with a flat row tip.

Typical weld zone microstructures for the flat row tip, for sections taken both parallel and perpendicular to the vibration direction, are shown in Fig. 10, with a higher magnification view of the area indicated in blue shown in Fig. 11. It is evident from the full anvil and tip imprints that both coupons were securely gripped during welding. The

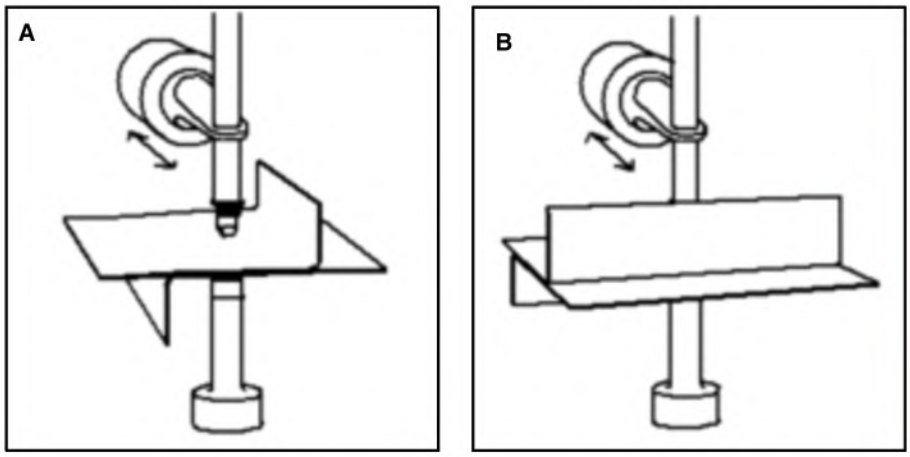

Fig. 4 — Test direction relative to vibration input direction – tensile-shear samples: A — Perpendicular; B — parallel.

Table 1 — Microstructural Feature Designations

Symbol	Microstructural Feature
A1	Side thickness – top sheet thickness adjacent to welded area
A2	Side gap – vertical gap between upper and lower specimens adjacent to welded area
A3	Side angle – angle between upper and lower specimens adjacent to welded area
B1	Indent width – width of welder tip imprint, measured at base of indents
B2	Weld diameter – horizontal distance between the unwelded gaps at the edge of the weld zone
C1	Tip peak-valley – vertical distance between tip peaks and valleys
C2	Tip side-valley – vertical distance between unwelded surface and tip valley imprints
C3	Tip side-peak – vertical distance between unwelded surface and tip peak imprints
D1	Anvil peak-valley – vertical distance between anvil peaks and valleys
D2	Anvil side-valley – vertical distance between unwelded surface and anvil valley imprints
D3	Anvil side-peak – vertical distance between unwelded surface and anvil peak imprints
E1	Weld thickness – average thickness of the welded region of the sample
F1	Weld thickness, tip side – vertical distance between the weld zone centerline and the tip indents
F2	Weld thickness, anvil side – vertical distance between the weld zone centerline and the anvil indents
G1	Wake left – vertical height of the leftmost wake feature
G2	Wake right – vertical height of the rightmost wake feature
G3	Wake 1 – vertical height of the 1st of the 3 most prominent wake features within the body of the weld
G4	Wake 2 – vertical height of the 2nd of the 3 most prominent wake features within the body of the weld
G5	Wake 3 – vertical height of the 3rd of the 3 most prominent wake features within the body of the weld

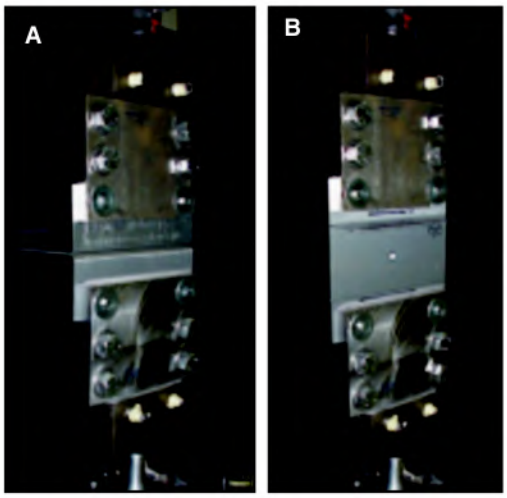

Fig. 5 — Samples mounted for tensile testing: A — T-peel sample; B — tensile-shear sample.

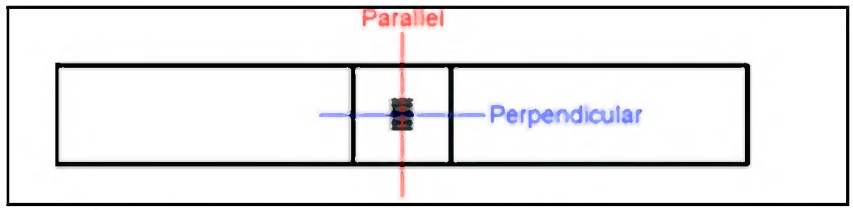

Fig. 6 — Weld section schematic (welds sectioned at weld centerline).

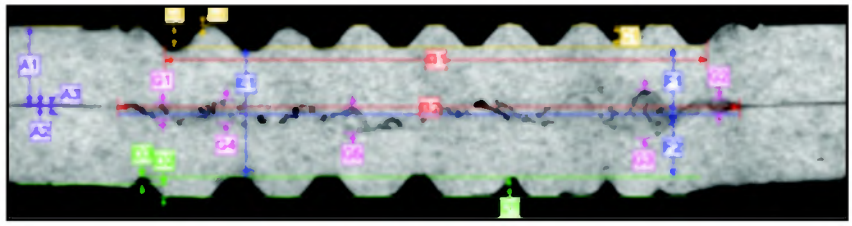

Fig. 7 — Measurement of weldment microstructural features.

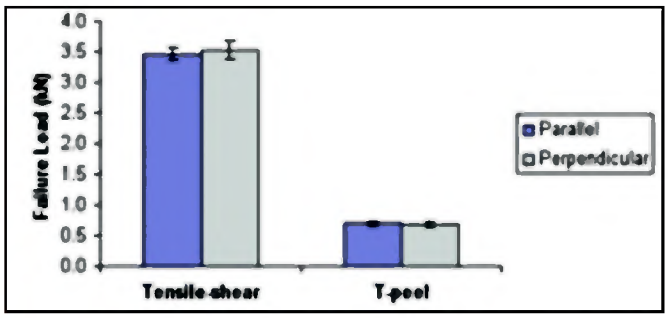

Fig. 8 — Tensile-shear and T-peel weld failure load as a function of test direction.

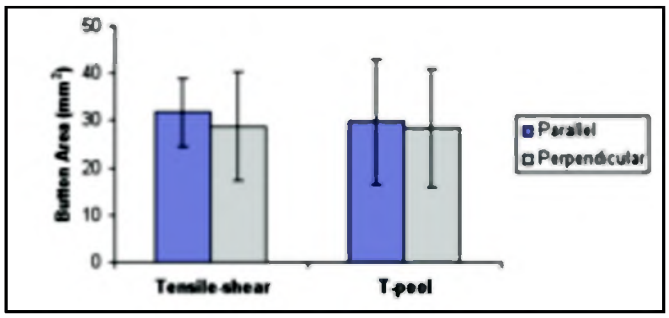

Fig. 9 — Button size as a function of test type and test direction.

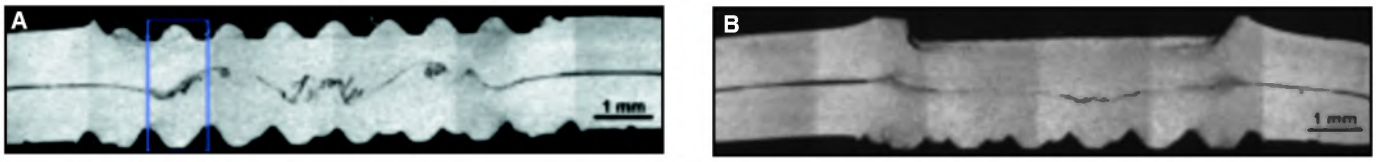

Fig. 10 — Ultrasonic weld microstructure as a function of cut direction: A — Cross section taken parallel to vibration direction; B — cross section taken perpendicular to vibration direction.

interfacial wake features almost completely span the width of the tip contact area. Other than some grain elongation near the tip and anvil contact interfaces and some submicron size grain refinement directly adjacent to the displaced interface, there is no notable difference in grain structure between the welded and unwelded regions of the samples. In the perpendicular weld cross section, more material displacement above the top surface of the coupon is apparent.

As detailed previously, 19 microstructural features were used to characterize ultrasonic weldability as a function of weld orientation and component rolling direction. It should be noted that microstructural measurements are sensitive to cross-sectional cut location; mounting, polishing, and etching procedures; and operator-to-operator variation in feature selection. Nevertheless, numerous conclusions can be drawn with respect to microstructural feature correlations with weld strength and the responses of microstructural features to changes in study factors.

For the welding parameter ranges used in this study, higher tensile-shear and T-peel failure loads were associated with larger weld diameters, better gripping of the weldment surface, reduced tip penetration, thicker weld regions, an offset of the weld zone toward the anvil side, and larger wake feature amplitudes. With the exception of average wake feature amplitudes (i.e., the average of the amplitudes of the five measured wake features, G1–G5), when welding with the flat row tip, these microstructural features were not appreciably influenced by cross section orientation, sheet rolling direction alignment, or orientation of the top sheet rolling direction relative to the vibration direction (additional detail regarding these latter two factors is provided in the next section). Wake feature amplitudes, conversely, were found to be significantly greater for parallel cross sections and for welds in which the rolling directions of the two sheets being welded were aligned. Because test direction and sheet rolling direction were not found to significantly impact ultrasonic weld strength, however, it was concluded that while there may be a moderate correlation between larger wake structures and higher weld failure loads, the relationship does not appear to be causal.

Robustness to Aluminum Sheet Rolling Direction

Objective

Ultrasonic weldability is a function of many variables, including component

material properties, geometry, and fixturing. This study was designed to assess process robustness to one of these variables — material properties, and more specifically, sheet rolling direction. In a production application, the orientation of a welding machine with respect to the rolling lines on a component can vary greatly. It is also possible for the relative orientation of the rolling directions of the two components being joined to vary. Mitskevich (Ref. 7) found that when welding with a flat tip at small vibration amplitudes, if the rolling lines of sheets were aligned, weld shear strengths could be 25% higher than if they were perpendicular to one another. De Vries (Ref. 8) noted the possibility that surface roughness variations as a function of aluminum sheet rolling direction might impact ultrasonic weldability, but did not conduct experiments to address this issue. The objective of this study, therefore, was to ascertain whether the orientation of a welding machine with respect to the rolling lines on a sheet component or the relative orientation of the rolling directions of two components being joined is critical.

Fig. 11 — Higher magnification image of location indicated in Fig. 10.

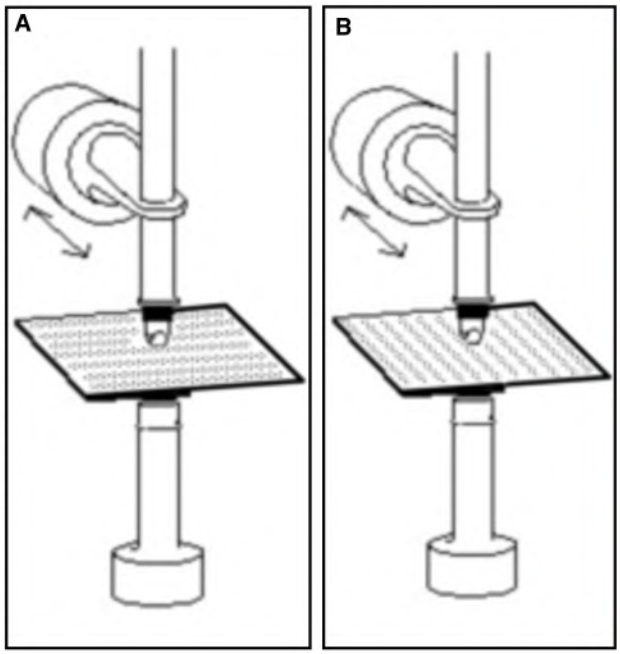

Fig. 12 — Orientation of top sheet rolling direction with respect to vibration direction: A — Perpendicular; B — parallel.

Experimental Procedure

Two scenarios, intended to frame the range of potential welding scenarios, were investigated for each of the rolling line factors. In the case of welder orientation with respect to the rolling lines on a component, welds were made with either the top sheet rolling direction perpendicular to the welding vibration direction (Fig. 12A) or the top sheet rolling direction parallel to the welding vibration direction — Fig. 12B. With respect to the relative orientation of the rolling directions of the two sheets being joined, this study examined the possibility of both alignment between the two sheets (Fig. 13A) and lack of sheet alignment — Fig. 13B. The experimental procedure was otherwise as detailed in the prior section.

Results

Again, results presented focus on those specific to the flat row tip. DOE analyses indicated that tensile-shear and T-peel failure loads and button areas were not appreciably impacted by the orientation of the top sheet rolling direction relative to the vibration direction or the relative orientation of the rolling directions of the two sheets. Figure 14 illustrates these findings, depicting failure load data as averaged, in each case, across all other factors. Error bars correspond to ±1 standard deviation.

While tensile-shear and T-peel weld failure loads were not appreciably impacted by component rolling direction, weld duration was. The voltage and current time profiles measured during welding were used to determine weld duration, i.e., the length of time during which ultrasonic electrical power was delivered to the welding machine. Weld duration was shortest when the rolling directions of the two sheets were aligned and when the rolling direction of the top sheet was parallel to the vibration input direction, as shown in Fig. 15. There were no statistically significant correlations (Pearson or Spearman's rank) at the 95% confidence level, however, between weld failure load or button area and weld duration for either the tensile-shear or T-peel specimens.

Robustness to Residual Stamping Lubricant Level

Objective

Prior work has indicated that the surface condition of aluminum workpieces can affect their ultrasonic weldability. Mitskevich (Ref. 7) reviewed literature relevant to the impact of workpiece surface preparation on resultant weld strength and found that precleaning of aluminum workpieces could significantly increase bond strength and reduce its variability for a given set of weld conditions. Equivalent weld strength could be achieved in cleaned and uncleaned pieces, if additional ultrasonic energy was expended. Weare et al. (Ref. 9) found that cleaning affected the interfacial appearance of fractured aluminum welds. Harthoorn (Ref. 10) found that the presence of lubricant on the surface of aluminum sheet influenced weld formation as did the mechanical abrasion of sheet surfaces prior to welding. Daniels (Ref. 11) determined that the surface condition of workpieces could significantly impact ultrasonic weld strength, but Mitskevich (Ref. 7) found that mechanically finishing workpiece surfaces (e.g., grinding, burring) prior to welding did not affect resultant weld strength in a consistent fashion.

Often, in North American automotive production facilities, components are not cleaned prior to welding. Rather, parts are welded with residual stamping lubricant on the surfaces. Nominal applied surface lubricant levels (i.e., 1 g/m^2) can be altered as a function of stamping and have been measured to be in the range of 0.1–1 g/m^2 at the time of welding. As such, a study was undertaken to determine whether the same weld parameters could produce good welds at both low and high lubricant levels.

Experimental Procedure

Experiments were conducted to determine the effects of surface lubricant level on ultrasonic weld strength, fatigue performance, and microstructural features for AA6111-T4 and AA5754 sheet. All welding was conducted using a Sonobond pedestal welding machine operated with uniform welding parameters. For each alloy, all coupons were cut from the same batch of material and ultrasonically

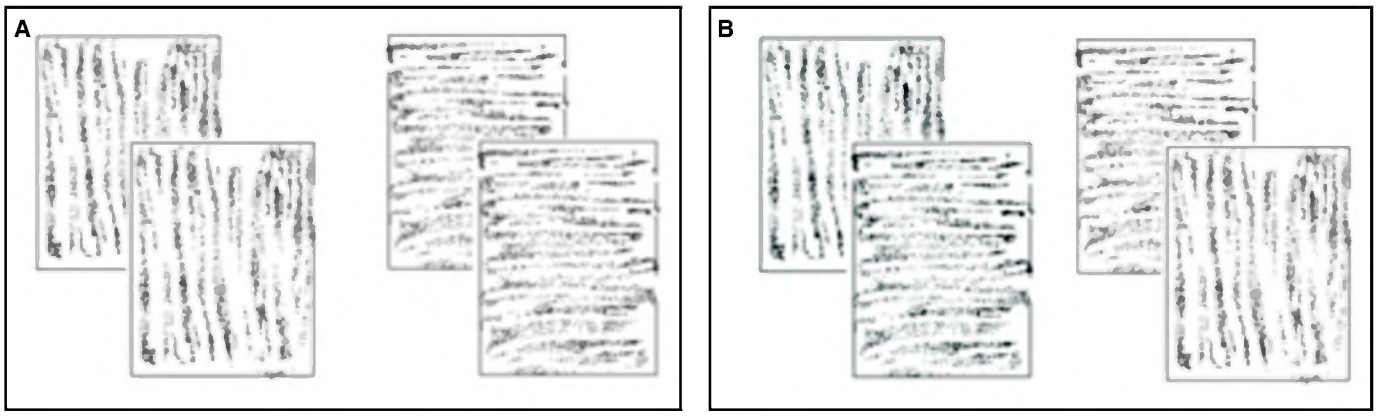

Fig. 13 — Relative orientation of rolling directions of two sheets: A — Sheets aligned; B — sheets not aligned.

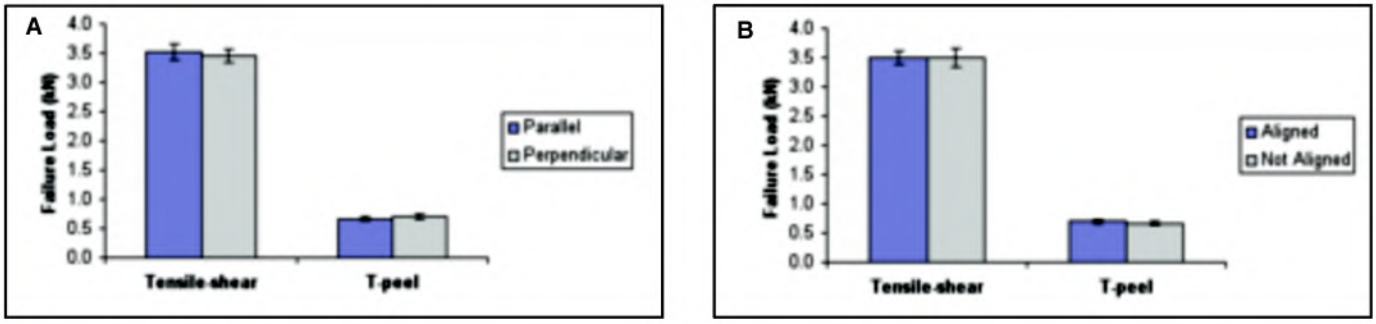

Fig. 14 — Tensile-shear and T-peel weld failure loads as a function of sheet rolling direction: A — Top sheet rolling direction orientation relative to vibration input direction; B — alignment of the rolling directions of the two sheets being joined.

cleaned in hexane prior to the controlled application of MP404 lubricant using a robotic sprayer. Three lubricant levels were evaluated as representative of actual production: 0.3, 0.6, and 1 g/m^2 MP404. Sample dimensions were 100 × 25 × 0.9 mm for the AA6111 coupons and 100 × 25 × 1.0 mm for the AA5754 coupons.

Forty-two AA6111 samples and 35 AA5754 samples were evaluated at each lubricant level — 9 replicates in tensile-shear and T-peel for each alloy; 3 via microstructural analysis for AA6111; and either 21 or 17 in fatigue for AA6111 (7 load levels) and AA5754 (6 load levels), respectively. T-peel samples were welded with 100% overlap and bent after welding but before paint-baking. All other samples were welded in a lap joint configuration with 25-mm overlap. To ensure consistent weldment geometry, samples were welded using a sample holding fixture. After welding, all samples were baked at 165°C for 20 min to emulate a typical automotive paint-bake cycle. Tensile-shear and T-peel testing were conducted using an Instron Model 55R1125 with a crosshead speed of 10 mm/min. Fatigue testing was conducted using an MTS closed-loop servo-hydraulic test machine with a 458 controller. A stress ratio (R) of 0.1 was employed, and testing was conducted at frequencies ranging from 1 to 30 Hz, with slow frequencies employed at the higher loads and higher frequencies at the low loads. For each weld cross section, 19 microstructural features were measured to characterize weld dimensions, tip and anvil imprints, and base material deformation, as previously detailed in Table 1 and Fig. 7.

Results

Figure 16 displays tensile-shear and T-peel failure loads as a function of lubricant level for the AA6111 and AA5754 ultrasonic welds. All four data sets — AA6111 and AA5754 tensile-shear and T-peel — exhibited homogeneity of variance, means, and medians at the 95% confidence level as a function of lubricant level. Figure 17 shows the fatigue performance of the AA6111 and AA5754 ultrasonic spot welds. Variations as a function of lubricant level were minimal. The data indicate that the strength and fatigue performance of 0.9-mm AA6111 and 1.0-mm AA5754 ultrasonic spot welds are robust to variations in residual stamping lubricant over the range of 0.3 to 1.0 g/m^2. In addition, no significant variations in the 19 measured microstructural features as a function of lubricant level were found. Migration of the lubricant was not explicitly evaluated in this study, but related work (Ref. 12) indicates that the lubricant is displaced from the welded region.

Robustness to Material Age

Objective

AA6111 is an Al-Mg-Si heat-treatable aluminum alloy designed for outer body applications. It is typically delivered to stamping facilities in the T4 condition in order to minimize forming difficulties, such as springback, during stamping operations. After forming and subsequent welding operations, components undergo artificial aging via a paint bake cycle. The paint bake cycle subjects the material to elevated temperature for a controlled time period, thereby stabilizing properties and resulting in increased yield stress and hence improved dent resistance. The T4 temper involves solution heat treatment followed by rapid quenching. After quenching, 6xxx series alloys can continue to age-harden for long periods of time at room temperature (Ref. 13). It is well known that material-to-material hardness variations affect ultrasonic weldability, and Kearns (Ref. 14) indicates that the energy required to make an ultrasonic weld is a function of the hardness of the material being welded. As such, this study was intended to determine the impact, if any, of coil age (i.e., shelf life post manufacture date) of AA6111-T4 on ultrasonic weldability.

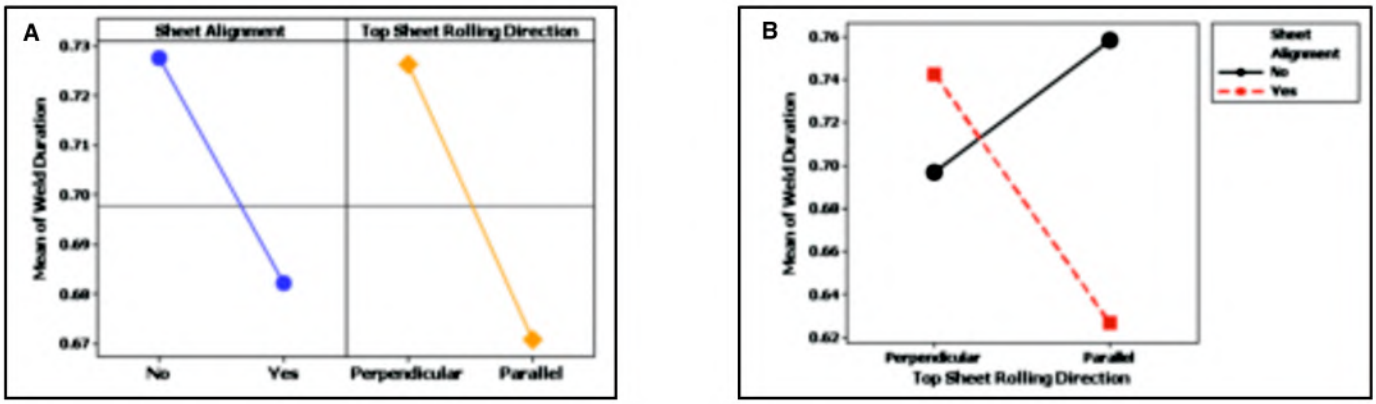

Fig. 15 — Effect of aluminum sheet rolling direction on weld duration: A — Main effects; B — two-factor interactions.

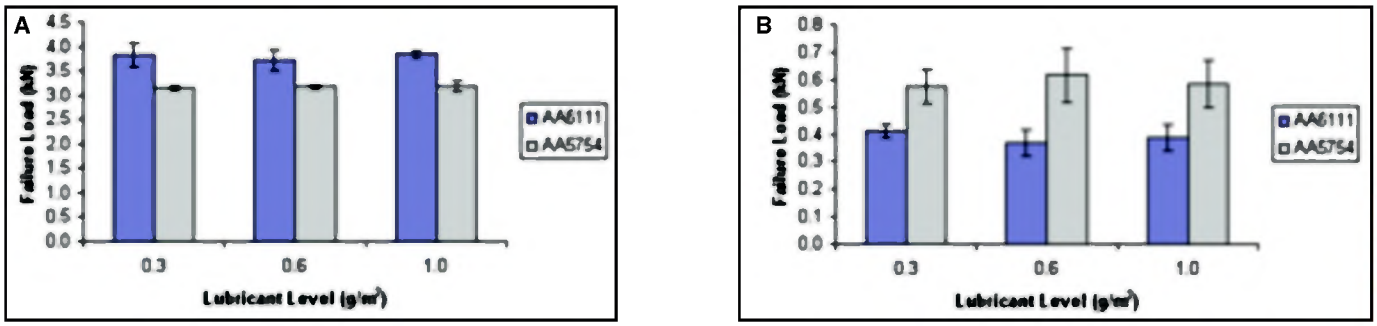

Fig. 16 — AA6111 and AA5754 tensile-shear and T-peel failure loads as a function of lubricant level: A — Tensile-shear; B — T-peel.

Experimental Procedure

A Branson Linear20 lateral-drive system was used to ultrasonically weld 100 × 25 × 0.9 mm AA6111-T4 coupons in both tensile-shear and T-peel configurations. All material was taken from the same material coil, with a production date of 4/8/06. Weldability testing was initiated on 8/8/06, with subsequent testing at three (11/8/06), six (2/1/07), and twelve (8/1/07) month intervals, corresponding to material ages of ~4, 7, 10, and 16 months, respectively. On the first three of the aforementioned dates, sets of 20 welds were made for both tensile-shear and T-peel testing. On the fourth date (8/1/07), due to limited material availability, sets of only 18 welds were made for both tensile-shear and T-peel testing. All samples were baked at 165°C for 20 min after welding to simulate a typical automotive paint bake cycle. Tensile-shear and T-peel testing were conducted using an Instron Model 55R1125 with a crosshead speed of 10 mm/min.

Results

Figure 18 displays tensile-shear and T-peel failure load data as a function of material age at time of welding. The boxplots of Fig. 18 depict first (Q1) and third (Q3) quartile lines, median lines, mean values (indicated by crosshair symbols), and outliers (indicated by asterisk symbols). Upper whisker lines extend to the highest data value within the upper limit (Q3+1.5[Q3–Q1]), and lower whisker lines extend to the lowest value within the lower limit (Q1–1.5[Q3–Q1]). Of the four data sets, the 7-month data are characterized by the greatest level of scatter, the lowest average tensile-shear failure load, and the highest average T-peel failure load. The 4-, 10-, and 16-month data appear similar to one another.

Statistical analyses were conducted to characterize the normality of the tensile-shear and T-peel data sets and to compare means, medians, and variances. Anderson-Darling tests for normality indicated that only four of the eight data sets followed normal distributions at the 95% confidence level. It is expected that all of the data would follow normal distributions if sample sizes were increased.

Variance equality was tested using F-tests, Bartlett's tests, and Levene's tests. Bartlett's tests and F-tests, which replace

Table 2 — P-Values for Tensile-Shear Data Mean/Median Comparisons, with Blue Numbers Indicating Mean/Median Equality at the 95% Confidence Level

	4 months		7 months		10 months		16 months	
	T-test	K-W	T-test	K-W	T-test	K-W	T-test	K-W
7 months	0.00	0.00	—	—	—	—	—	—
10 months	0.00	0.00	0.00	0.00	—	—	—	—
16 months	**0.15**	**0.37**	0.00	0.00	**0.19**	**0.20**	—	—

Table 3 — P-Values for T-Peel Data Mean/Median Comparisons, with Blue Numbers Indicating Mean/Median Equality at the 95% Confidence Level

	4 months		7 months		10 months		16 months	
	T-test	K-W	T-test	K-W	T-test	K-W	T-test	K-W
7 months	0.00	0.00	—	—	—	—	—	—
10 months	**0.70**	**0.52**	0.00	0.00	—	—	—	—
16 months	**0.10**	**0.18**	0.00	0.00	**0.09**	**0.53**	—	—

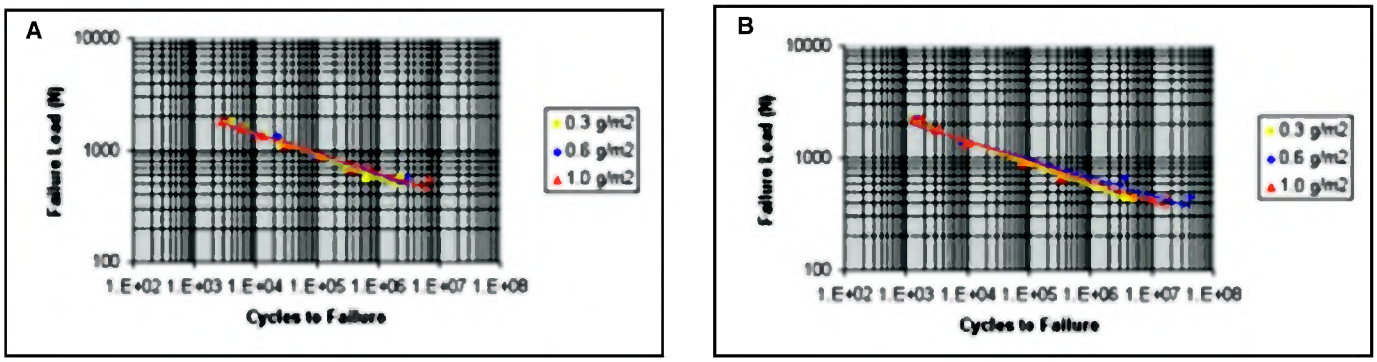

Fig. 17 — Fatigue performance as a function of lubricant level: A — AA6111; B — AA5754.

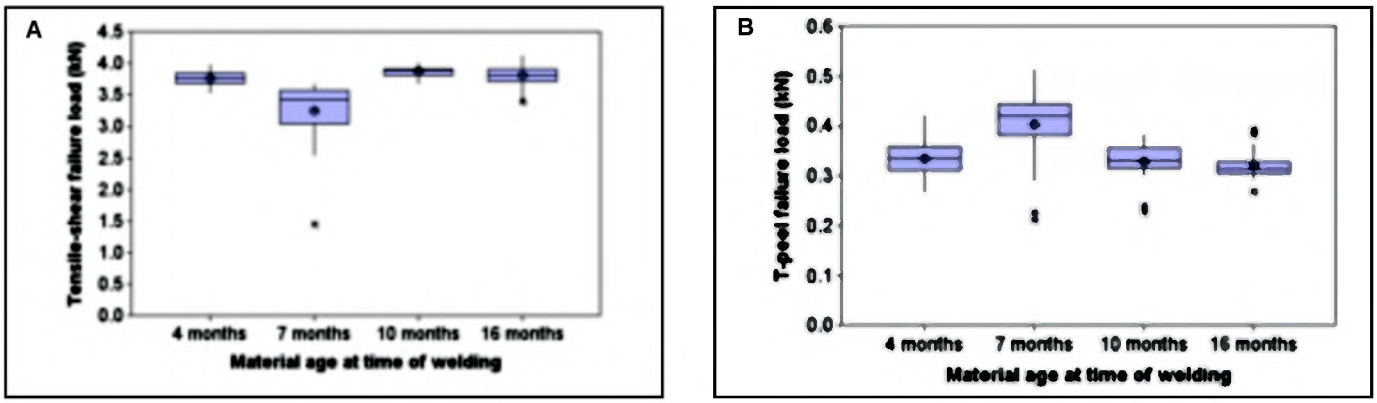

Fig. 18 — Failure load as a function of material age at time of welding: A — Tensile-shear; B — T-peel.

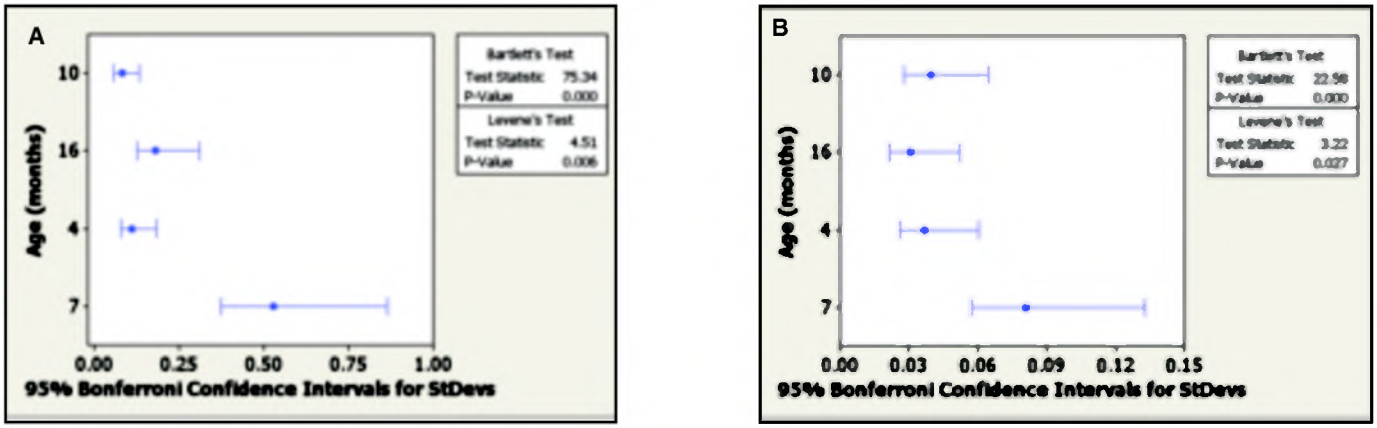

Fig. 19 — Test for variance equality. Failure load as a function of material age at time of welding: A — Tensile-shear; B — T-peel.

Bartlett's tests when there are only two levels, assume that the data come from normal distributions, while Levene's test simply assumes that the data come from continuous, but not necessarily normal, distributions. Levene's test considers the distances of the observations from their sample median rather than their sample mean. Figure 19 displays Bonferroni confidence intervals for the standard deviation and Bartlett's and Levene's test results for variance equality for the tensile-shear and T-peel data. Both Bartlett's and Levene's tests indicate variance inequality for the tensile-shear and T-peel data. The Bonferroni 95% confidence intervals for the standard deviations display significant overlap between the 4-, 10-, and 16-month samples for both the tensile-shear and T-peel data. The confidence interval for the 7-month data does not overlap with that of the other samples in the case of the tensile-shear data and only minimally overlaps with those of the other samples in the case of the T-peel data, indicating inequality of variance. Individual two-sample comparisons corroborate these findings.

Data medians were compared using the Kruskal-Wallis test, which provides a nonparametric alternative to the one-way analysis of variance (Ref. 15). Kruskal-Wallis does not assume that the data come from normal distributions. So, while the parametric test is more powerful (has a higher probability of rejecting the null hypothesis when it is false), Kruskal-Wallis is more robust against violation of the assumptions (normality and homogeneity of variance). Kruskal-Wallis assumes that samples are from continuous distributions and

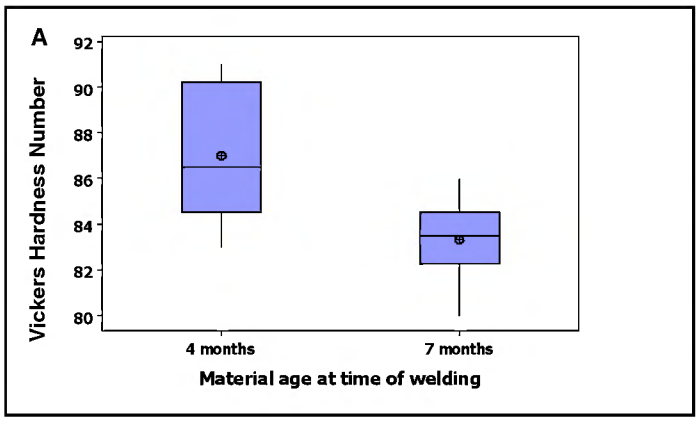

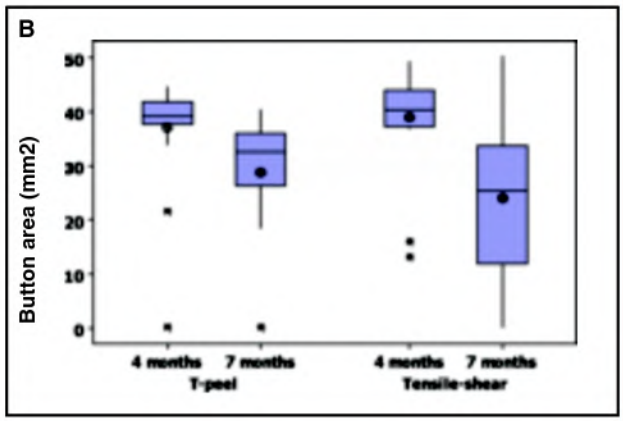

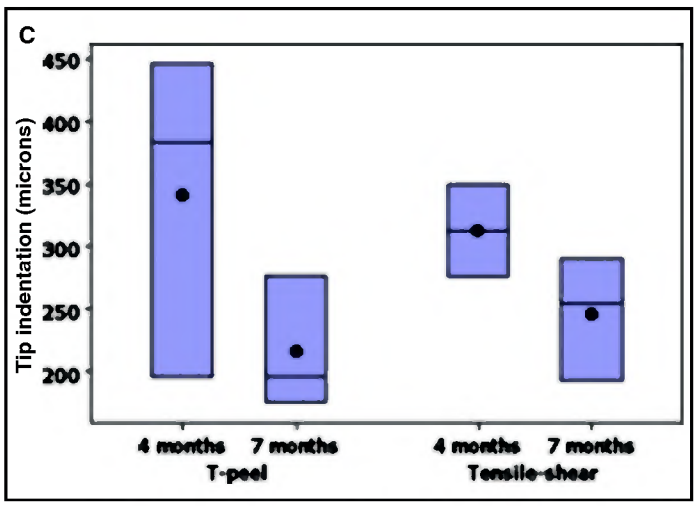

Fig. 20 — Characterization of potential noise factors in aging study: A — Vickers microhardness measurements as a function of sample batch; B — button size as a function of test type and material age at time of welding; C — tip indentation as a function of test type and material age at time of welding.

Fig. 21 — Button pull-out (left) and interfacial fracture (right) failure modes.

examines the equality of medians of the samples. Kruskal-Wallis analyses of the tensile-shear and T-peel data indicate that there are statistically significant differences at the 95% confidence level between the data medians, as a function of material age at time of welding.

Individual, two-sample comparisons were conducted to further elucidate differences between data sets. Tables 2 and 3 display the p-values associated with two sample T-tests and Kruskal-Wallis (K-W) tests between each pair of tensile-shear and T-peel data, with data sets exhibiting equality of means (in the case of the T-test) or medians (in the case of the Kruskal-Wallis test) at the 95% confidence level identified via blue highlight. Two-sample T-tests examine the difference between sample means of unknown variance; for smaller samples, they work best if data are from normal distributions. In both Tables 2 and 3, results from the T-tests and the Kruskal-Wallis tests are in agreement. In the case of the tensile-shear data (Table 2), the 16-month data means and medians are indistinguishable from the 4- and 10-month values. In the case of the T-peel data (Table 3), the 4-, 10-, and 16-month data are identical at the 95% confidence level with respect to mean/median values. As was the case with the variances, the 7-month data set stands out as the anomaly.

Increases in yield strength in heat treatable aluminum alloys due to age hardening are a continuous function of time over time periods significantly longer than 16 months (Ref. 13). As such, it can be concluded that the anomalous data at the 7-month mark in this study is likely attributable to an irregularity in the experimental procedure, rather than a true variation in ultrasonic weldability as a function of material age. It should be noted that potential sources of error which were controlled during this study were material (all material was from the same coil), specimen size (all coupons were sheared to nominally identical dimensions), and welding parameters. As such, principal outstanding sources of variation might include welding tool mount, welder operation, and postweld bake cycle.

The possibility of variations in the temperature and/or duration of the bake cycle to which samples were subjected after welding was assessed using material hardness measurements. Vickers microhardness testing was conducted on two coupons each from the 4- and 7-month batches (Fig. 20A), at a location remote from the weld site. It should be noted that prior work (Ref. 1) has revealed no evidence of significant hardness variation between the weld region and the base metal for ultrasonic spot welds in 6XXX series aluminum. A statistically significant difference in mean hardness values (and hence material yield stress, Ref. 16) at the 95% confidence level was determined for this small sample set, but the ~4% change in hardness values cannot alone account for the ~14% change in tensile-shear failure load.

Weld failure morphology was also examined as a potential factor for the anomalous data at the 7-month material age, in

particular because the 7-month data are characterized by lower tensile-shear strength but higher T-peel strength. All 20 tensile-shear samples and 19 of the 20 T-peel samples welded at 4 months material age failed via button pull-out, as depicted in Fig. 21. The alternative failure mode is interfacial fracture and is also depicted in Fig. 21. Eighteen of the 20 samples welded at 7 months material age failed via button pull-out in both tensile-shear and T-peel. Button shape was quite consistent throughout. Button area as a function of material age at time of welding is shown in Fig. 20B for both tensile-shear and T-peel samples. The T-peel data displayed homogeneity of variances at the 95% confidence level, but the tensile-shear data demonstrated variance inequality as a function of material age. For both the tensile-shear and the T-peel data, there were statistically significant differences (p-value < 0.05) in mean and median button size as a function of material age at time of welding, with the decrease in mean tensile-shear button area being 70% greater than the decrease in mean T-peel button area. Tensile-shear button area correlated moderately well with tensile-shear failure load, but the T-peel data did not exhibit a similar statistically significant correlation.

Tip indentation was examined as a potential indicator of differences in welding machine operation between the data sets and hence explanation for the anomalous strength data at the 7-month material age. While tip indentation appears lower for the 7-month data as shown in Fig. 20C, the difference was not statistically significant.

In summary, while a comprehensive evaluation of all potential noise factors contributing to the anomalous strength data at the 7-month material age is not possible post experiment, the aforementioned analyses do indicate the existence of slight irregularities in the experimental procedure associated with that experimental batch. Microhardness variations indicate post-weld bake cycle inconsistencies that are in line with the observed 7-month weldment strength disparities. Differences in tip indentation and tensile-shear and T-peel button sizes also indicate that welding machine operation and/or welding tool mount may have been dissimilar for the 7-month data set. Therefore, as previously stated, it was concluded that the anomalous data at the 7-month mark in this study is due to an irregularity in the experimental procedure, rather than a true variation in ultrasonic weldability as a function of material age.

Conclusions

Requisite to the implementation of ultrasonic metal welding in automotive body construction applications is demonstration of process robustness to manufacturing variables. In this study, process robustness to four critical issues — weld orientation, aluminum sheet rolling direction, residual stamping lubricant level, and material age — has been established. Ultrasonic weld tensile-shear and T-peel failure loads and button sizes were not found to vary significantly as a function of weld orientation. Despite the directional nature of the energy input by linear ultrasonic welding systems, weld strength was essentially equivalent parallel to and perpendicular to the vibration input direction. In addition, tensile-shear and T-peel failure loads and button areas were not appreciably impacted by the orientation of the top sheet rolling direction relative to the vibration direction or the relative orientation of the rolling directions of the two sheets being joined. While weld duration was influenced by component rolling direction, there were no statistically significant correlations between weld failure load or button area and weld duration for either the tensile-shear or T-peel specimens. Ultrasonic weld strength, fatigue performance, and microstructural features for 0.9-mm AA6111 and 1.0-mm AA5754 sheet were determined to be robust to variations in residual stamping lubricant (MP404) over the range of 0.3 to 1.0 g/m^2. Finally, coil age in the range of 4 to 16 months was not found to impact the ultrasonic weldability of AA6111-T4, as characterized using tensile-shear and T-peel weld failure loads. In summary, ultrasonic metal welding process robustness to weld orientation, aluminum sheet rolling direction, residual stamping lubricant level, and material age have been demonstrated. These findings are important for the implementation of ultrasonic metal welding in automotive body construction applications.

Acknowledgments

This work was supported in part by the U.S. National Institute of Standards and Technology's Advanced Technology Program under Cooperative Agreement No. 70NANB3H3015. The authors would like to thank Ron Cooper for conducting the microhardness measurements and Al Krause for carrying out the fatigue testing.

References

1. Hetrick, E., Jahn, R., Reatherford, L., Skogsmo, J., Ward, S., Wilkosz, D., Devine, J., Graff, K., and Gehrin, R. 2005. Ultrasonic spot welding: A new tool for aluminum joining. *Welding Journal* 84(2): 26–30.

2. Jones, J. B., and Powers, J. J. Jr. 1956. Ultrasonic welding. *Welding Journal* 35(8): 761–766.

3. Jones, J. B., Elmore, W. C., and De Prisco, C. F. 1960. Method and apparatus employing vibratory energy for bonding metals. Aeroprojects Inc., Assignee. U.S. Patent 2,946,119.

4. Ultrasonic metal welding — enabling the all aluminum vehicle. 2003. NIST ATP Award No. 70NANB3H3015. *http://jazz.nist.gov/atpcf/prjbriefs/prjbrief.cfm?ProjectNumber=00-00-5503*.

5. Tsujino, J., Sano, T., Ogata, H., Tanaka, S., and Harada, Y. 2002. Complex vibration ultrasonic welding systems with large area welding tips. *Ultrasonics* 40: 361–364.

6. Jones, J. B., and Potthoff, W. C. 1959. Certain structural properties of ultrasonic welds in aluminum alloys. *Welding Journal* 38(7): 282-s to 288-s.

7. Mitskevich, A. M. 1973. Ultrasonic welding of metals. *Physical Principles of Ultrasonic Technology* Volume 1, trans. J. S. Wood. New York: Plenum Press. Originally published in L. D. Rozenberg, ed., *Fizicheskie osnovy ul'trazvukovoi tekhnologii* (Moscow: Nauka Press, 1970).

8. De Vries, E. 2004. Mechanics and mechanisms of ultrasonic metal welding. PhD diss., The Ohio State University.

9. Weare, N. E., Antonevich, J. N., and Monroe, R. E. 1960. Fundamental studies of ultrasonic welding. *Welding Journal* 39(8): 331-s to 341-s.

10. Harthoorn, J. L. 1978. Ultrasonic metal welding. PhD diss., Technische Hogeschool Eindhoven.

11. Daniels, H. P. C. 1965. Ultrasonic welding. *Ultrasonics* 3(4): 190–196.

12. Wilkosz, D. E. 2007. Bond formation in ultrasonically welded aluminum sheet metal. PhD diss., Stony Brook University.

13. Davis, J. R., ed. 1994. *Aluminum and Aluminum Alloys*. Materials Park, Ohio: ASM International.

14. Kearns, W. H., ed. 1980. *Welding Handbook*. Miami, Fla.: American Welding Society.

15. Sheskin, D. J. 1997. *Handbook of Parametric and Nonparametric Statistical Procedures*. New York, N.Y.: CRC Press, Inc.

16. Mott, B. W. 1956. *Micro-Indentation Hardness Testing*. London: Butterworths Scientific Publications.